Electrochemical Characteristics of a Self-Propagating Molecular-Based Assembly†

Leila Motiei,‡ Michal Lahav,‡ Antonino Gulino,⊥ Mark A. Iron,§ and Milko E. van der Boom*,‡

Departments of Organic Chemistry and Chemical Research Support, The Weizmann Institute of Science, 76100 Rehovot, Israel, and Department of Chemistry, University of Catania, 95125 Catania, Italy

Received: November 16, 2009; Revised Manuscript Received: December 23, 2009

The electrochemical properties of a metallosupramolecular network that undergoes reversible redox chemistry on indium−tin oxide (ITO)-coated glass substrates have been investigated. The redox-active osmium complexes are electrochemically accessible even for films with a thickness > 15 nm. The electrochemical data correlates well with our previously observed self-propagating growth process, for which the electron density for the assemblies remains constant during film growth. Electron-transfer rate constants obtained by potential step chronoamperometry experiments suggest an exceptionally low attenuation factor, β, of 0.013 ± 0.001 Å^{-1}. However, the intrinsically porous nature of the assembly could be to a large extent or even entirely responsible for such a low value.

The electrochemical properties of surface-confined molecular-based materials have been a fascinating and active field of fundamental research for many decades and have generated significant debate.[1,2] The search for redox-active, electrochromic, and highly conductive materials offers the promise of new applications, including plastic electronics and organic photovoltaics.[3–5] However, device-quality systems are still uncommon. Many electrochemical studies with polymers, polyelectrolytes, mono- and multilayered films, and other solid-state structures have been devoted to elucidate details regarding structure−function relationships and electron-transfer properties.[6–8] The molecular structures used vary widely and range from bioinspired systems and complex organic materials to redox-active complexes on various conducting surfaces (e.g., gold, doped silicon, and indium−tin oxide (ITO)-coated glass).

We recently reported on the formation and electrochromic behavior of metal−organic networks consisting of robust polypyridyl osmium complexes (**1**) cross-linked by $PdCl_2$ (Figure 1).[4,9] The characterization of these coordination-based assemblies includes UV/vis spectroscopy, synchrotron X-ray reflectivity (XRR), X-ray photoelectron spectroscopy (XPS), and ellipsometry. During the assembly process, palladium salt is stored in the already-formed assembly and this reservoir is used in the formation of the additional layers in an exponential manner. These self-propagating assemblies undergo significant and reversible optical changes when exposed to an electric current.[4] The high density of redox-active metal complexes may make such materials suitable candidates for battery technology[10] and may result in a system capable of generating H_2 and O_2 from water.[11] Polypyridyl complexes akin to complex **1** have been studied in detail.[3,11–14] However, little is known about the electrochemical characteristics and electron-transfer properties of our self-propagating assemblies.[4,9] These properties are discussed here.

The cyclic voltammograms (CVs) of the assemblies show well-defined surface waves characteristic of an $Os^{2+/3+}$couple (Figure 2a).[14] The half-wave redox potential, $E_{1/2}$, is about 0.91 V versus Ag/AgCl, and the full widths at half-maximum (fwhm) are 150 ± 10 mV regardless of the thickness. These fwhm values are larger than the ideal value of 90.6 mV, suggesting some degree of lateral interaction between the osmium complexes and/or a heterogeneous distribution of the redox centers.[15,16] Please note that for lateral interactions between osmium centers to occur, density functional theory (DFT) calculations (vide infra) show that the electrons have to breach a gap of 27.21 Å. Such interactions have been observed in other films consisting of similar polypyridyl complexes.[13] The peak-to-peak separation, ΔE_p, increases with both the film thickness and the scan rate, ν, (Figures 2a and S1, Supporting Information), indicating a slower electron-transfer process under these conditions. Up to a film thickness of 9.4 nm, the peak current is directly proportional to ν within the range of 0.01−1 V s^{-1}, indicating a surface-confined process that is not limited by diffusion (Figure 2b).[17] For thicker films (>15 nm), the peak currents scale linearly with $\nu^{1/2}$, suggesting relatively slow ion diffusion into the film (Figure S2, Supporting Information). The total oxidation charge, Q, estimated by integration of the voltammetric peaks, increases exponentially with the number of deposition steps (Figure 2c). However, Q scales linearly with film thickness, demonstrating that approximately equal densities of complex **1** are deposited while maintaining structural regularity (Figure 2d). These correlations are in good agreement with our previously observed self-propagating growth process, for which the electron density for the assemblies terminated with complex **1** ($\rho = 0.41$ e Å^{-3}, derived from synchrotron XRR measurements) remains constant.[9] In addition, the linear trend of Q versus film thickness demonstrates that the redox-active complexes are electrochemically accessible even for films with a thickness > 15 nm. The estimated surface coverage, Γ, ranges from 1.4×10^{-10} mol/cm^2 for the template layer to 3.5×10^{-9} mol/cm^2 for a 15 nm thick assembly. These values compare well with the surface coverage derived from UV/vis spectroscopy (Figure S3, Supporting Information).

We attempted to obtain electron-transfer rate constants, k, in the thin film assemblies using the Laviron model by measuring

† Part of the "Michael R. Wasielewski Festschrift".

* To whom correspondence should be addressed. E-mail: milko.vanderboom@weizmann.ac.il.

‡ Department of Organic Chemistry, The Weizmann Institute of Science.

§ Department of Chemical Research Support, The Weizmann Institute of Science.

⊥ University of Catania.

10.1021/jp910898f
Published on Web 01/20/2010

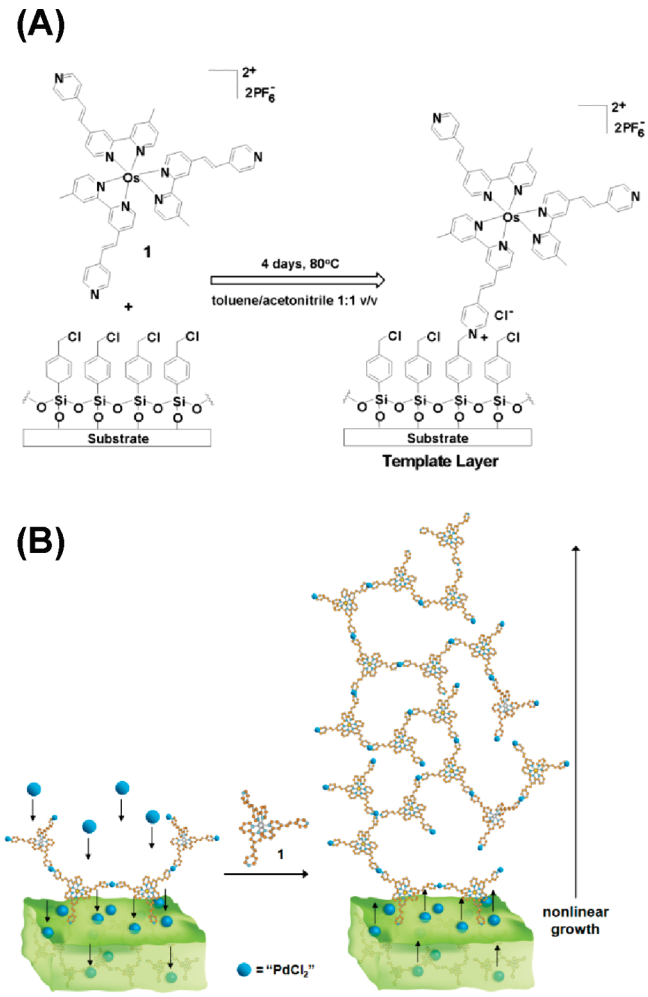

Figure 1. Self-propagating assembly. (A) The template layer was generated by treating a functionalized ITO electrode with a MeCN solution of the osmium polypyridyl complex **1** at an elevated temperature for several days. One of the pyridine groups underwent a quaternization process with a benzylchloride unit, as shown by X-ray photoelectron spectroscopy (XPS). (B) The coordination-based structure was formed on the template layer by iterative deposition of complex **1** and $(PhCN)_2PdCl_2$. Identical procedures for both (A) and (B) were used as described in ref 9.

the variation of peak potentials as a function of $\log(\nu)$.[18] The plots of anodic (E_{pa}) and cathodic (E_{pc}) peak potentials versus $\log(\nu)$ yield straight lines with $R^2 > 0.98$ (Figure S4, Supporting Information). The transfer coefficients, α, were derived from the slopes of the linear regimes $RT/\alpha nF$ and $RT/(1-\alpha)nF$ of the cathodic and anodic plots, respectively. The α values decrease from 0.32 to 0.076 during the buildup of the assemblies (Table S1, Supporting Information). Realistically, higher α values (the ideal value is 0.5) are needed to accurately derive k, and hence, it would seem that this model does not apply to our system. Low and decreasing α values with increasing film thickness are not uncommon and are indicative of disorder and/or defects.[19–21]

Potential step chronoamperometry (CA) experiments were next performed to estimate k using the expression: $I_{(t)} = kQ \exp(-kt)$.[22–24] A series of six samples were evaluated with thicknesses ranging from 1.6 to 9.4 nm, and all show monoexponential (or at least one strongly dominant exponential) decay for the current response versus time (Figure S5, Supporting Information). An example for a 6.5 nm thick film with $k = 154$ s^{-1} is shown in Figure 3a. The electrolyte concentration does have an effect on k. For instance, the rate constant of a 2.5 nm thick film increases by ~4 fold by changing the concentration of $^nBu_4NBF_4$ in dry CH_3CN from 0.05 to 0.5 M, indicating the influence of ion pairing on the electron-transfer process (Figure S6, Supporting Information). The expression $k = k^\circ \exp(-\beta d)$ has been used to derive the attenuation factor, β. This formula gives the distance dependence of k, where k° and k are the standard rate constants at the bare and modified electrodes, respectively, and d is the film thickness. A good linear correlation ($R^2 = 0.98$) of $\ln(k)$ versus d was obtained with a slope of 0.013 ± 0.001 $Å^{-1}$ (Figure 3b). Such small values have been interpreted as β by others.[5,25–28] In particular, redox-active molecular wires on gold surfaces have been reported with remarkable electron-transport capabilities. Rampi conducted electrical conductivity experiments with these surface-bound oligomers using a Au/film/Hg setup,[25] while Nishihara used CA measurements.[29] Their data analysis resulted in extraordinary structure−property correlations, as expressed by small values for β ranging from 0.001 to 0.028 $Å^{-1}$. These values are much smaller than those observed for most films and solution-based systems[20,21,30–33] and have been attributed to the use of embedded metal centers.[25,29]

Does our assembly on ITO also qualify as an ultralow-β material? We believe that this is not the case, even though our value falls well within the range accepted in the recent literature.[25,29] The here-observed conductivity is apparently a function of many variables and includes both "real" and "defect-mediated" components that are difficult to separate. The basic elements of both our assemblies and the above-mentioned ultralow-β materials are cationic polypyridyl complexes; therefore, similar properties are to be expected. However, the intrinsically porous nature of our system could be to a large extent or even entirely responsible for the observed low β value.

CV measurements for a 6.5 nm thick assembly with different electrolytes (e.g., $^nBu_4NBF_4$, NH_4PF_6, $^nBu_4NCF_3SO_3$, and $^nBu_4NSO_3C_6H_4CH_3$) show minor effects indicating that the nature of counterion does not significantly change the charge transport (Figure S7, Supporting Information). For a highly porous material, this seems to be not unexpected as the pore size is likely larger than any of the counteranions used. Angle-resolved XPS provides important structural information that might explain the electrochemical observations. The porous nature of these films is apparent from the exposure of these films to a solution of $(PhCN)_2PdCl_2$ or $(NH_4)_2[Ce(NO_3)_6]$.[4,9] The XPS measured atomic ratios reveal that the excess palladium or cerium is stored in the assembly. For instance, the amount of cerium is highest at the top of the structure (Ce/Pd = 4.85), but a significant amount equal to twice the palladium content is found close to the substrate surface (Table S2, Supporting Information). The self-propagating assemblies are clearly permeable and most probably allow the incorporation of the electrolyte into the structure to maintain charge neutrality. It is highly likely that the low α and β values originate from the porous structure of the assemblies. It is noteworthy that Bard and co-workers have shown that pinholes can result in rate constants that are 3−4 orders of magnitude higher than those of defect-free films.[34] In addition, structural reorganization of the assemblies might occur during electrochemical measurements, as has recently been shown by Kraatz for redox-active monolayers.[35] The polypyridyl complexes are cross-linked by up to three Pd−pyridine bonds;[9] however, these bonds are not very strong (33 kcal/mol).[36]

DFT calculations were carried out on a model complex to give some insight into the structural and electronic properties

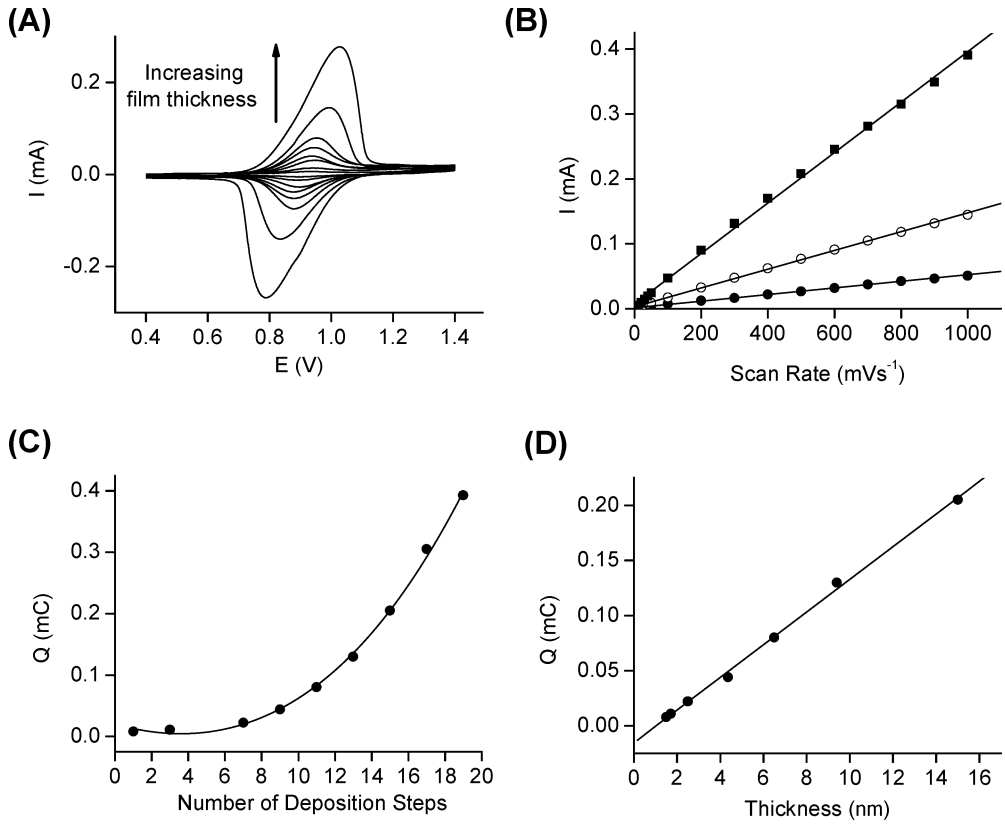

Figure 2. Representative electrochemical data. (A) Cyclic voltammograms of the assemblies terminated with a layer of complex **1** at a scan rate of 0.1 V s^{-1}. The data are shown for assemblies having the following thicknesses: 1.5, 1.7, 2.5, 4.3, 6.5, 9.4, 31, and 35 nm. (B) Peak current dependence of scan rates extracted from cyclic voltammograms for 1.5 (●), 2.5 (○), and 9.4 nm (■) thick assemblies. (C) Exponential increase, $R^2 = 0.98$, of the charge, Q_{mc}, versus the number of deposition cycles. (D) Linear dependence, $R^2 = 0.98$, of the charge, Q_{mc}, versus the film thickness. The film thickness has been determined by synchrotron X-ray reflectivity measurements (XRR) using silicon substrates.[9] Please note that the template layer is included in the number of deposition steps.

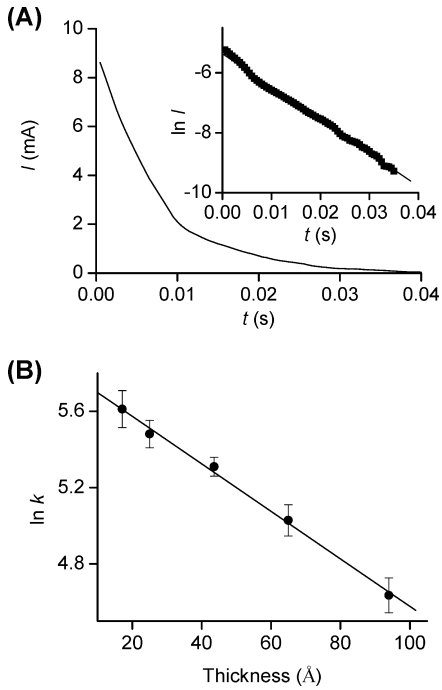

Figure 3. Potential step chronoamperometry (CA) experiments. (A) Current response, *I*, of an ITO electrode modified with a 6.5 nm thick assembly using a potential step of 0−1.8 V (0.1 M $^nBu_4NBF_4$ in dry CH_3CN). A large-amplitude potential step was used to avoid any complications from an *iR* drop across the modified films. (Inset) Semilogarithmic plot for the corresponding current response ($R^2 = 0.98$). (B) Plot of ln *k* versus the film thickness with $R^2 = 0.98$.

of the system (see the Supporting Information for details). In order to make the calculations more tractable, two of the modified bipyridyl ligands of complex **1** were replaced with unsubstituted 4,4′-bipyridine (bpy). Both the monomeric complex **1′** and the **1′**−$PdCl_2$−**1′** dimer were examined. The optimized structures are depicted in Figure S8 (Supporting Information). In the dimer, the Os−Pd and Os−Os distances are 13.61 and 27.21 Å, respectively. The HOMO, LUMO, and adjacent orbitals are shown in Figure S9 (Supporting Information). The HOMO and HOMO−1 are localized on the $PdCl_2$ unit, while the HOMO−2, LUMO, and LUMO+1 are delocalized over the $PdCl_2$ and osmium centers and the connecting bis(pyridylethylene) ligands. The DFT HOMO−LUMO gap is 2.35 eV, considerably smaller than the gap of 3.06 eV in the monomeric osmium complex. Regardless of the electron-transfer mechanism in the assembly, the transport has to take place over significant distances. In addition, even a fully formed metal−organic network based on complexes (**1**) bridged by $PdCl_2$ are likely to be permeable.

In conclusion, the high density of cationic, redox-active metal complexes could contribute to the charge-transfer characteristics of the assemblies, but it is more likely that the inherent porous structure plays a dominant role. Defects and pinholes are known to be the primary causes of an overestimation of the electron-transfer parameters.[6,34,37–39] Whether dynamic behavior of our metal−organic network during the electrochemical measurements plays a role remains an open question. Despite the above-mentioned reports on ultralow-β materials, we believe that the electrochemical characteristics of our system yield structural

information of the assemblies rather than the electron-transfer rates of the molecular components. The electrochemical data is in agreement with the electrochromic properties, while the porous structure of the self-propagating self-assembly provides accessibility to all of the redox sites in the assembly. These observations indicate that these assemblies are promising candidates for the storage of various compounds, separation, and size-selective sensing.[40]

Experimental Section

Materials and Methods. ITO-coated glass slides ($7 \times 50 \times 0.7$ mm, $R_s = 5-15\ \Omega/\square$) were obtained from Delta Technologies. Tetrabutylammonium tetrafluoroborate ($TBABF_4$) and anhydrous CH_3CN ($H_2O < 0.001\%$ v/v) were purchased from Aldrich. The preparation of the osmium complex (**1**) and the procedure for the stepwise assembly of films has been published elsewhere.[9]

Electrochemical Measurements. Cyclic voltammetry and chronoamperometry were performed using a potentiostat (CHI660A) connected to a personal computer. All measurements were performed in a three-electrode cell configuration consisting of (i) an ITO-modified substrate (working electrode), (ii) a Pt wire (counter electrode), and (iii) Ag/AgCl (a reference electrode). The experiments were performed at room temperature using 0.1 M solutions of $TBABF_4$ in dry CH_3CN, unless stated otherwise. RC cell time constants, estimated as the fastest components in the current decay during chronoamperometric measurements, were shorter than 2 ms. The interfacial kinetics were measured only at times greater than 2−5 RC.

Acknowledgment. This research was supported by the Helen and Martin Kimmel Center for Molecular Design, the G. M. J. Schmidt Minerva Center, and the Weizmann−U.K. joint research program.

Supporting Information Available: Electrochemical measurements (Figures S1−S7 and Table S1), optical (UV/vis) spectroscopy (Figure S3), XPS data (Table S2), and computational details (Figure S8). This material is available free of charge via the Internet at http://pubs.acs.org.

References and Notes

(1) Chidsey, C. E. D. *Science* **1991**, *251*, 919–922.
(2) Balzani, V. *Electron Transfer in Chemistry*; Wiley-VCH: Weinheim, Germany, 2001.
(3) Hagfeldt, A.; Gratzel, M. *Acc. Chem. Res.* **2000**, *33*, 269–277.
(4) Motiei, L.; Lahav, M.; Freeman, D.; van der Boom, M. E. *J. Am. Chem. Soc.* **2009**, *131*, 3468–3469.
(5) Davis, W. B.; Svec, W. A.; Ratner, M. A.; Wasielewski, M. R. *Nature* **1998**, *396*, 60–63.
(6) Haran, A.; Waldeck, D. H.; Naaman, R.; Moons, E.; Cahen, D. *Science* **1994**, *263*, 948–950.
(7) Joachim, C.; Gimzewski, J. K.; Aviram, A. *Science* **2000**, *408*, 541–548.
(8) Carter, M. T.; Rowe, G. K.; Richardson, J. N.; Tender, L. M.; Terrill, R. H.; Murray, R. W. *J. Am. Chem. Soc.* **1995**, *117*, 2896–2899.
(9) Motiei, L.; Altman, M.; Gupta, T.; Lupo, F.; Gulino, A.; Evmenenko, G.; Dutta, P.; van der Boom, M. E. *J. Am. Chem. Soc.* **2008**, *130*, 8913–8915.
(10) Astruc, D.; Ornelas, C.; Ruiz, J. *Chem.—Eur. J.* **2009**, *15*, 8936–8944.
(11) Youngblood, W. J.; Lee, S.-H. A.; Maeda, K.; Mallouk, T. E. *Acc. Chem. Res.* **2009**, *42*, 1966–1973.
(12) Gupta, T.; van der Boom, M. E. *Angew. Chem., Int. Ed.* **2008**, *47*, 5322–5326.
(13) Walsh, D. A.; Keyes, T. E.; Hogan, C. F.; Forster, R. J. *J. Phys. Chem. B* **2001**, *105*, 2792–2799.
(14) Gupta, T.; Cohen, R.; Evmenenko, G.; Dutta, P.; van der Boom, M. E. *J. Phys. Chem. C* **2007**, *111*, 4655–4660.
(15) Chidsey, C. E. D.; Bertozzi, C. R.; Putvinski, T. M.; Mujsce, A. M. *J. Am. Chem. Soc.* **1990**, *112*, 4301–4306.
(16) Li, J.; Wang, L.; Liu, J.; Evmenenko, G.; Dutta, P.; Marks, T. J. *Langmuir* **2008**, *24*, 5755–5765.
(17) Shiryaeva, I. M.; Collman, J. P.; Boulatov, R.; Sunderland, C. *J. Anal. Chem.* **2003**, *75*, 494–502.
(18) Laviron, E. *J. Electroanal. Chem.* **1979**, *101*, 19–28.
(19) Finklea, H. O.; Avery, S.; Lynch, M.; Furtsch, T. *Langmuir* **1987**, *3*, 409–413.
(20) Hong, H. G.; Mallouk, T. E. *Langmuir* **1991**, *7*, 2362–2369.
(21) Katz, E.; Itzhak, N.; Willner, I. *Langmuir* **1993**, *9*, 1392–1396.
(22) Katz, E.; Willner, I. *Langmuir* **1997**, *13*, 3364–3373.
(23) Forster, R. J.; Faulkner, L. R. *J. Am. Chem. Soc.* **1994**, *116*, 5444–5452.
(24) Forster, R. *J. Anal. Chem.* **1996**, *68*, 3143–3150.
(25) Tuccitto, N.; Ferri, V.; Cavazzini, M.; Quici, S.; Zhavnerko, G.; Licciardello, A.; Rampi, M. A. *Nat. Mater.* **2009**, *8*, 41–46.
(26) Sedghi, G.; Sawada, K.; Esdaile, L. J.; Hoffmann, M.; Anderson, H. L.; Bethell, D.; Haiss, W.; Higgins, S. J.; Nichols, R. J. *J. Am. Chem. Soc.* **2008**, *130*, 8582–8583.
(27) Goldsmith, R. H.; Sinks, L. E.; Kelley, R. F.; Betzen, L. J.; Liu, W.; Weiss, E. A.; Ratner, M. A.; Wasielewski, M. R. *Proc. Natl. Acad. Sci. U.S.A.* **2005**, *102*, 3540–3545.
(28) Sikes, H. D.; Smalley, J. F.; Dudek, S. P.; Cook, A. R.; Newton, M. D.; Chidsey, C. E. D.; Feldberg, S. W. *Science* **2001**, *291*, 1519–1523.
(29) Nishimori, Y.; Kanaizuka, K.; Kurita, T.; Nagatsu, T.; Segawa, Y.; Toshimitsu, F.; Muratsugu, S.; Utsuno, M.; Kume, S.; Murata, M.; Nishihara, H. *Chem.—Asian J.* **2009**, *4*, 1361–1367.
(30) Akkerman, H. B.; Blom, P. W. M.; de Leeuw, D. M.; de Boer, B. *Nature* **2006**, *441*, 9–72.
(31) Salomon, A.; Cahen, D.; Lindsay, S.; Tomfohr, J.; Engelkes, V. B.; Frisbie, C. D. *Adv. Mater.* **2003**, *15*, 1881–1890.
(32) Giacalone, F.; Segura, J. L.; Martin, N.; Guldi, D. M. *J. Am. Chem. Soc.* **2004**, *128*, 5340–5341.
(33) He, J.; Chen, F.; Li, J.; Sankey, O. F.; Terazono, Y.; Herrero, C.; Gust, D.; Moore, T. A.; Moore, A. L.; Lindsay, S. M. *J. Am. Chem. Soc.* **2005**, *127*, 1384–1385.
(34) Kiani, A.; Alpuche-Aviles, M. A.; Eggers, P. K.; Jones, M.; Gooding, J. J.; Paddon-Row, M. N.; Bard, A. J. *Langmuir* **2008**, *24*, 2841–2849.
(35) Orlowski, G. A.; Chowdhury, S.; Kraatz, H.-B. *Langmuir* **2007**, *23*, 12765–12770.
(36) Ray, L.; Shaikh, M. M.; Ghosh, P. *Dalton Trans.* **2007**, 4546–4555.
(37) Finklea, H. O., In *Electroanalytical Chemistry*; Bard, A. J., Ed.; Marcel Dekker: New York, 1996; Vol. 19, pp 109−335.
(38) Weiss, E. A.; Chiechi, R. C.; Kaufman, G. K.; Kriebel, J. K.; Li, Z.; Duati, M.; Rampi, M. A.; Whitesides, G. M. *J. Am. Chem. Soc.* **2007**, *129*, 4336–4349.
(39) Finklea, H. O.; Snider, D. A.; Fedyk, J.; Sabatani, E.; Gafni, Y.; Rubinstein, I. *Langmuir* **1993**, *9*, 3660–3667.
(40) Belanger, S.; Hupp, J. T. *Angew. Chem., Int. Ed.* **1999**, *38*, 2222–2224.

JP910898F